PHYSICAL REVIEW B **80**, 161311(R) (2009)

Local density of states in disordered two-dimensional electron gases at high magnetic field

Thierry Champel
Laboratoire de Physique et Modélisation des Milieux Condensés, CNRS and Université Joseph Fourier, Boîte Postale 166, 25 Avenue des Martyrs, 38042 Grenoble Cedex 9, France

Serge Florens
Institut Néel, CNRS and Université Joseph Fourier, Boîte Postale 166, 25 Avenue des Martyrs, 38042 Grenoble Cedex 9, France

(Received 6 October 2009; published 28 October 2009)

Motivated by high-accuracy scanning tunneling spectroscopy measurements on disordered two-dimensional electron gases in strong magnetic field, we present an expression for the local density of states (LDoS) of electrons moving in a smooth arbitrary potential landscape on the scale of the magnetic length, that can be locally described up to its second derivatives. We use a technique based on coherent-state Green's functions, allowing us to treat on an equal footing confining and open quantum systems. The energy dependence of the LDoS is found to be universal in terms of local geometric properties, such as drift velocity and potential curvature. We also show that thermal effects are quite important close to saddle points, leading to an overbroadening of the tunneling trajectories.

DOI: 10.1103/PhysRevB.80.161311 PACS number(s): 73.43.−f, 73.20.At

The most remarkable feature of the quantum Hall effect[1] lies perhaps in the fundamental role played by local imperfections for the successful observation of perfectly quantized Hall conductance plateaus in two-dimensional electron gases (2DEG) at high perpendicular magnetic field. Yet, many physical aspects of these systems related to spatial disorder, which are crucial to understand, e.g., the nature of the quantum Hall transitions, are not easily elucidated from macroscopic measurements. For this reason, many experimental works were devoted in recent years toward developing local probes,[2] and have unveiled surprisingly rich interplays of disorder and electronic interactions. The most straightforward local measurement in interpretative terms is certainly the local density of states (LDoS) obtained from the scanning tunneling spectroscopy (STS). Such experiments are however impeded by the fact that 2DEG are usually buried several hundreds of nanometers below the sample surface, while the characteristic length scale of the quantum Hall regime, the so-called magnetic length $l_B=\sqrt{\hbar c/|e|B}$, with $\hbar$ Planck's constant, c the speed of light, $e=-|e|$ the electron charge, and B the magnetic field strength, ranges about 10 nanometers at fields of several Teslas. Only very recently could STS spectra be obtained with an accuracy comparable to l_B, thanks to a special surface treatment of InSb semiconductors.[3] This experiment has shown that localized electronic states of an incompressible quantum Hall fluid follow closed semiclassical cyclotron orbits, with a spatial smearing on the scale l_B due to wave-function broadening. Near saddle points of the disordered potential landscape, wider structures were observed, that were linked to quantum tunneling.

In this Rapid Communication, we propose a simple analytical theory for the electronic LDoS in a smooth arbitrary potential landscape and strong, yet finite, perpendicular magnetic field, on the basis of a coherent-state Green's function formalism.[4,5] As a guide to experimentalists, we provide simple analytical expressions for the energy-dependent LDoS, and distinguish qualitative spectral features according to whether thermal or quantum smearing prevails. In the latter case, different line shapes are obtained for nonzero or vanishing drift velocity. We also show that thermal broadening is much more effective near saddle points, and may contribute to the broad structures observed in Ref. 3.

Focusing on incompressible regions of quantum Hall systems, we consider the single-particle Hamiltonian for a charged particle confined to a two-dimensional $\mathbf{r}=(x,y)$ plane in the presence of both a perpendicular magnetic field and an arbitrary potential-energy landscape V,

$$H=\frac{1}{2m^*}\left(-i\hbar\boldsymbol{\nabla}_{\mathbf{r}}-\frac{e}{c}\mathbf{A}(\mathbf{r})\right)^2+V(\mathbf{r}), \tag{1}$$

with the vector potential $\mathbf{A}$ defined by $\boldsymbol{\nabla}\times\mathbf{A}=B\hat{\mathbf{e}}_z$ and m^* the electron effective mass. The STS spectra at fixed energy ε are proportional to the temperature (T) broadened local density of states,[6]

$$\rho^{\mathrm{STS}}(\varepsilon,\mathbf{r},T)=\frac{-1}{\pi}\mathrm{Im}\int d\omega\frac{G(\mathbf{r},\mathbf{r},\omega)}{4T\cosh^2[(\omega-\varepsilon)/2T]} \tag{2}$$

obtained from the retarded Green's function $G(\mathbf{r},\mathbf{r}',\omega)$ of Hamiltonian (1). This quantity can be systematically expanded in a power series of the type $l_B^{n_x+n_y}\partial_x^{n_x}\partial_y^{n_y}V(\mathbf{r})$, as was shown in Ref. 5. This can be done by introducing the Landau-level index m together with a continuous quantum number $\mathbf{R}=(X,Y)$ defining the "vortex"-like singularity of the following family of coherent states:

$$\langle\mathbf{r}|m,\mathbf{R}\rangle=\frac{1}{\sqrt{2\pi l_B^2 m!}}\left(\frac{z-Z}{\sqrt{2}l_B}\right)^m e^{-(|z|^2+|Z|^2-2Zz^*)/(4l_B^2)} \tag{3}$$

with $z=x+iy$ and $Z=X+iY$. Modified vortex state Green's functions $h_m(\mathbf{R})$ can then be obtained,[5] which read for simplicity in the limit of vanishing Landau-level mixing [$\omega_c=|e|B/(m^*c)\to\infty$, but keeping l_B finite],

$$G(\mathbf{r},\mathbf{r},\omega)=\sum_{m=0}^{+\infty}\int\frac{d^2\mathbf{R}}{2\pi l_B^2}|\Phi_m(\mathbf{R}-\mathbf{r})|^2 h_m(\mathbf{R}), \tag{4}$$

$$|\Phi_m(\mathbf{R})|^2=\frac{1}{\pi m!\, l_B^2}\frac{\partial^m}{\partial s^m}\left.\frac{e^{-A_s\mathbf{R}^2/l_B^2}}{1+s}\right|_{s=0} \tag{5}$$

with $A_s=(1-s)/(1+s)$. It can be checked[7] by inspection that, up to second spatial derivatives of the potential, Dyson equation for the Green's function exactly maps onto the following partial differential equation

$$1=\left[\omega+i0^+-E_m-V(\mathbf{R})-\frac{2m+1}{4}l_B^2\Delta_{\mathbf{R}}V\right]h_m(\mathbf{R}) + \frac{l_B^4}{8}[\partial_Y^2V\partial_X^2+\partial_X^2V\partial_Y^2-2\partial_X\partial_YV\partial_X\partial_Y]h_m(\mathbf{R}), \tag{6}$$

with $\Delta_{\mathbf{R}}$ the Laplacian operator.

We give here a brief account of previous works on high magnetic field calculations, emphasizing similarities and differences to the present analysis. The popular semiclassical guiding center picture obtained at $l_B\to 0$ keeps a quantum treatment of fast cyclotron motion only, and leads to eigenenergies that are discrete with respect to the Landau-level index m but continuous with the external potential (a precise mathematical formulation was given in Refs. 5 and 8). Our quantum approach naturally contains this semiclassical limit, as seen by keeping the first line of Eq. (6) only, so that $h_m(\mathbf{R})$ is indeed given by a simple pole, shifted by a $V(\mathbf{R})$-dependent term from the energy $E_m=(m+1/2)\omega_c$ of isolated Landau levels. With this result, Green's function G naturally encodes that the wave functions are translation-invariant Landau states with drift velocity $c\boldsymbol{\nabla}V(\mathbf{r})\times\hat{\mathbf{e}}_z/(|e|B)$, mathematically vindicating an early idea by Trugman.[9] Capturing quantization/dissipation respectively for closed/open systems asks however for a full quantum treatment of the guiding center, embodied in the second line of Eq. (6). The technique of projection onto the lowest Landau level at finite l_B developed in Ref. 10 bears in this respect more similarities to ours. However, the formalism of Ref. 10 leads to the resolution of a one-dimensional Schrödinger equation for the wave function, while the present analysis is based on Green's functions for the overcomplete set of states $|m,\mathbf{R}\rangle$. As a result, an expression such as Eq. (4) is quite powerful for an *arbitrary* potential $V(\mathbf{r})$ that is locally well described by its Taylor expansion, as this does not rely on a cumbersome parametrization of the equipotential lines, as required for a complete set of wave functions. We note that the path-integral formalism developed in Ref. 11 and also based on the use of the states [Eq. (3)] seems to suffer from technical difficulties that were not elucidated, so that general expressions for observables such as the LDoS, to be discussed in this Rapid Communication, were not obtained to our knowledge. Also, the inclusion of Landau-level mixing is there challenging, in contrast to extensions of our Green's function formalism.[5]

Equation (6) is now easily solved by a mapping onto an ordinary differential equation thanks to the redefinition $h_m(\mathbf{R})=f_m[E(\mathbf{R})]$, where $E(\mathbf{R})=V(\mathbf{R})-V(\mathbf{R}_0)$, with $\mathbf{R}_0$ an arbitrary reference point for now:

$$1=\left[(\tilde{\omega}_m+i0^+-E)+(\gamma E+\eta)\frac{d^2}{dE^2}+\gamma\frac{d}{dE}\right]f_m(E), \tag{7}$$

where

$$\tilde{\omega}_m=\omega-E_m-V(\mathbf{R}_0)-(m+1/2)\zeta, \tag{8}$$

$$\gamma=\frac{l_B^4}{4}\mathrm{Det}[H_V]|_{\mathbf{R}=\mathbf{R}_0}, \tag{9}$$

$$\eta=\frac{l_B^4}{8}[(\boldsymbol{\nabla}V\times\hat{\mathbf{e}}_z)\cdot H_V(\boldsymbol{\nabla}V\times\hat{\mathbf{e}}_z)]|_{\mathbf{R}=\mathbf{R}_0}, \tag{10}$$

$$\zeta=\frac{l_B^2}{2}\Delta_{\mathbf{R}}V|_{\mathbf{R}=\mathbf{R}_0}. \tag{11}$$

The coefficient γ is proportional to the determinant of the Hessian matrix $[H_V]_{ij}=\partial_i\partial_jV$ with $i,j=\{X,Y\}$. Its sign determines the geometrical nature of the critical points at which the gradient of V vanishes (a saddle point is characterized by $\gamma<0$, while $\gamma>0$ indicates the presence of a local extremum). Physically remarkable is the loose analogy of Eq. (7) to damped Newtonian dynamics of equipotential lines with a friction coefficient given by $-\gamma$. This consideration already shows that dissipation, i.e., deviation from a simple pole structure for $h_m(\mathbf{R})$, will thus occur at the saddle points of $V(\mathbf{r})$.

Differential Eq. (7) is second order in the derivative with respect to E, but linear in E. By doing a Fourier transform to time t, it will become quadratic in t and first order in the derivative with respect to t. Enforcing causality, one finds that the solution to Eq. (7) is

$$f_m(E)=-i\int_0^{+\infty}dt\frac{e^{-i(E+\eta/\gamma)\tau(t)}}{\cos(\sqrt{\gamma}t)}e^{i(\tilde{\omega}_m+i0^++\eta/\gamma)t}, \tag{12}$$

with $\tau(t)=(1/\sqrt{\gamma})\tan(\sqrt{\gamma}t)$. Both cosine and tangent trigonometric functions are replaced by their hyperbolic counterparts in the case $\gamma<0$. Equation (12) thus remarkably describes both closed and open quantum systems on an equal footing. When $\gamma>0$, $\tau(t)$ is a periodic function of time, so that $f_m(E)$ must display discrete poles, and one can recover, e.g., for a rotationally invariant quadratic potential the full solution of the Fock-Darwin problem at small Landau-level mixing.[7] In contrast, for $\gamma<0$, the spectrum remains continuous, as expected from the solution[12] for the saddle-point potential. Quite interestingly, the convergence of the integral in Eq. (12) for $\gamma<0$ is not ensured by the $\exp(-0^+t)$ cutoff function, but by the kernel $1/\cosh(\sqrt{-\gamma}t)$, with an energy scale $\sqrt{-\gamma}$ related to the curvature of the potential (see discussion below for the implications to the LDoS). This leads to the appearance of a finite imaginary part in the self-energy associated to the equipotential lines, hinting at quantum dissipation effects (see Ref. 7 for further discussion).

Because $h_m(\mathbf{R})=f_m[E(\mathbf{R})]$ obtained in Eq. (12) has a

simple exponential dependence on $E(\mathbf{R})$, it is possible to perform analytically the $\mathbf{R}$-integration in Eq. (4) by developing $V(\mathbf{R})$ to quadratic order around $\mathbf{R}_0=\mathbf{r}$. After doing the frequency integral in Eq. (2), the LDoS reads as

$$\rho^{\mathrm{STS}}(\varepsilon,\mathbf{r},T)=\frac{1}{2\pi l_B^2}\mathrm{Re}\sum_{m=0}^{+\infty}\frac{1}{m!}\frac{\partial^m}{\partial s^m}\int_0^{+\infty}dt\frac{Tt}{\sinh[\pi Tt]}\left.\frac{e^{i[\varepsilon-E_m-(m+1/2)\zeta-V(\mathbf{r})]t+i\eta/\gamma[t-\tau(t)]-[\tau^2(t)/4][A_s l_B^2|\nabla_{\mathbf{r}}V|^2+4i\eta\tau(t)]/[A_s^2+iA_s\zeta\tau(t)-\gamma\tau^2(t)]}}{(1+s)\cos(\sqrt{\gamma}t)\sqrt{A_s^2+iA_s\zeta\tau(t)-\gamma\tau^2(t)}}\right|_{s=0} \tag{13}$$

which is our final theoretical result, to be interpreted at the light of the STS measurements of Ref. 3. Although Eq. (13) is only exact (at small Landau-level mixing) for a generic quadratic external potential (in which case only η and $|\nabla_{\mathbf{r}}V|$ depend on $\mathbf{r}$), it constitutes[7] a very accurate approximation at finite T for an *arbitrary* potential that can be locally described by the site-dependent geometrical quantities $\{|\nabla_{\mathbf{r}}V|,\gamma(\mathbf{r}),\eta(\mathbf{r}),\zeta(\mathbf{r})\}$. Clearly, the function appearing in integral (13) is governed by several energy scales, associated to various broadening processes of the LDoS, that we review in turn (for simplicity, we focus on the lowest Landau level $m=0$).

Quantum smearing from drift motion. One notices first the appearance of the energy $\omega_{\mathrm{drift}}=l_B|\nabla_{\mathbf{r}}V(\mathbf{r})|$ associated with the drift velocity. When ω_{drift} is the largest energy scale, the smearing of the LDoS is dominated by the transverse width l_B of the Landau wave functions, and a good approximation to the LDoS is given by calculating (13) at $\gamma=\eta=T=0$:

$$\rho^{\mathrm{STS}}(\varepsilon,\mathbf{r},0)\approx\frac{1}{2\pi l_B^2}\frac{\exp\left\{-\left[\frac{\varepsilon-\omega_c/2-V(\mathbf{r})}{\omega_{\mathrm{drift}}}\right]^2\right\}}{\sqrt{\pi}\omega_{\mathrm{drift}}}. \tag{14}$$

The energy dependence via ε (controlled experimentally with a back gate voltage) is thus Gaussian in this regime, and is shown in Fig. 1. We assume for all plots given here the saddle-point potential profile

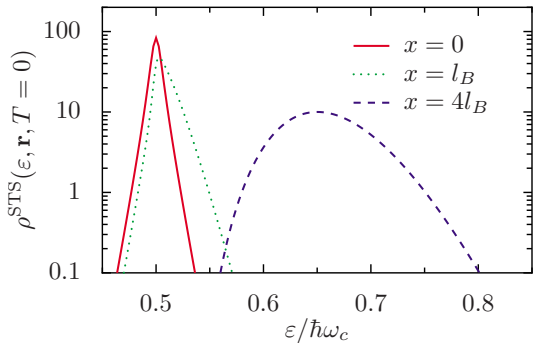

FIG. 1. (Color online) LDoS from Eq. (13) in units of $(2\pi l_B^2)^{-1}$ as a function of ε at $T=0$ for the saddle-point potential [Eq. (15)] with $\omega_0/\omega_c=0.1$. Here, three different positions were chosen along the bisecting line $x=y$: at the saddle point ($x=0$, left curve), in the crossover region ($x=l_B$, middle curve), and in the drift dominated region ($x=4l_B$, right curve).

$$V(\mathbf{r})=m^*\omega_0^2xy. \tag{15}$$

We note that small corrections to Eq. (14) from exact formula (13) provide spectral asymmetries related to the parameter η (see right curve in Fig. 1).

Quantum smearing from tunneling at saddle points. Expression (14) is certainly invalid at saddle points ($\mathbf{r}=0$) where ω_{drift} vanishes. If the energy $\omega_{\mathrm{saddle}}=2\sqrt{-\gamma}$ associated to curvature exceeds both ω_{drift} and T, the LDoS is then better approximated by performing integral (13) with $|\nabla_{\mathbf{r}}V|=T=0$ [we take $\zeta=0$ for simplicity, which is satisfied by potential (15)],

$$\rho^{\mathrm{STS}}(\varepsilon,\mathbf{r},0)\approx\frac{P_{-1/2+ia}(0)}{2\pi l_B^2}\frac{\mathrm{sech}\left(\frac{\varepsilon-\omega_c/2-V(\mathbf{r})}{\omega_{\mathrm{saddle}}/\pi}\right)}{\sqrt{2}\omega_{\mathrm{saddle}}}, \tag{16}$$

where $P_{-1/2+ia}(x)$ is the conical function of the first kind[13] and $a=(\varepsilon-\omega_c/2-V(\mathbf{r}))/\omega_{\mathrm{saddle}}$. One can deduce from this Eq. (16) that the energy-dependent LDoS has an exponential behavior near saddle points (see left curve of Fig. 1). *Local geometric properties of the disorder potential thus have qualitative fingerprints on the LDoS.*

Thermal smearing. When T exceeds both ω_{drift} and ω_{saddle}, the integral (13) is cut by the $1/\sinh(\pi Tt)$ kernel, and is well described by

$$\rho^{\mathrm{STS}}(\varepsilon,\mathbf{r},T)\approx\frac{1}{2\pi l_B^2}\frac{\mathrm{sech}^2\left(\frac{\varepsilon-\omega_c/2-V(\mathbf{r})}{2T}\right)}{4T}. \tag{17}$$

The crossover from the $T=0$ limit to this thermally broadened form [Eq. (17)] is shown in Fig. 2. These results are

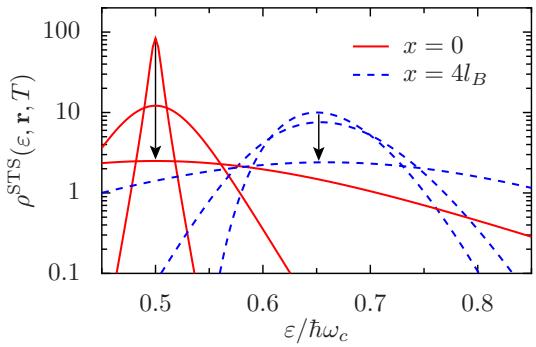

FIG. 2. (Color online) Thermal smearing of the same LDoS as shown in Fig. 1 for the positions $x=y=0$ and $x=y=4l_B$ only. Three different increasing temperatures $T/\omega_c=0,0.02,0.1$ were taken (top to bottom, along the arrows).

easily understood by the fact that typical values of ω_{drift} far from the saddle point are much larger than ω_{saddle}. For model potential (15) one has in particular $\omega_{\text{saddle}}=\omega_0^2/\omega_c \ll \omega_{\text{drift}}=\omega_{\text{saddle}}|\mathbf{r}|/l_B$ for $|\mathbf{r}| \gg l_B$. This means that *thermal smearing will be more effective near saddle points than onto the drift dominated orbits*, as clearly seen in Fig. 2.

This turns out to be a crucial observation for understanding the spatial dependence of the LDoS measured by Hashimoto *et al.*[3] Indeed, our results show that at $T=0$, the LDoS is sharply peaked, energetically and spatially, at the saddle points, so that only the tunneling trajectories that come very close should have appreciable intensity. However, in the intermediate temperature range $\omega_{\text{saddle}} \lesssim \pi T < \omega_{\text{drift}}$ [note the π prefactor difference in Eqs. (16) and (17)], important spatial redistribution of the spectral weight occurs at the saddle points so that tunneling structures broader than the magnetic length become visible, see the wide "bridge" connecting tunneling trajectories in Fig. 3 at finite temperature.

An important remark concerns how accurate Eq. (13) is for an *arbitrary* potential $V(\mathbf{r})$, since two assumptions were made in our derivation: (i) large Landau-level separation $\omega_c \gg l_B^2 \Delta_{\mathbf{r}} V$, i.e., $\omega_c \gg \omega_0$ for model (15); (ii) local description of $V(\mathbf{r})$ up to second-order spatial derivatives. Condition (i) is well satisfied in the experiments, as the analysis of the typical spatial variations of the LDoS maxima lead to a rough estimate $\omega_0 \lesssim 3$ meV, while $\omega_c = 70$ meV at $B = 12$ T for InSb. We also emphasize that Landau-level mixing corrections to all physical observables can be perturbatively accounted for in our formalism, as shown in Ref. 5 so that corrections due to finite ω_c are indeed small. In passing, we can also deduce from these experimental estimates the energy scale associated to curvature effects $\omega_0^2/\omega_c \lesssim 0.13$ meV. Since the base temperature $T=0.3$ K taken in Ref. 3 gives a thermal scale $\omega_{\text{thermal}}=\pi T \simeq 0.08$ meV, this seems consistent with our conclusions on the relevance of thermal smearing near saddle points. Requirement (ii) is actually satisfied provided that temperature exceeds the energy scales associated with third (and beyond) local derivatives of the potential, which turn out to be smaller than the curvature scale $\sim\sqrt{|\gamma|}$. We thus conclude that our Eq. (13) yields quantitative estimates for the LDoS of a weakly disordered electron gas at high but finite magnetic field.

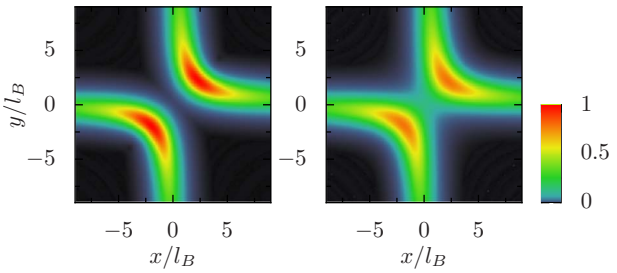

FIG. 3. (Color online) Spatial dependence of $\rho^{\text{STS}}(\varepsilon,\mathbf{r},T)$ (normalized to its maximal value at $T=0$) obtained from Eq. (13) for saddle-point potential (15), with $\omega_0/\omega_c=0.1$, $\varepsilon/\omega_c=0.54$, at $T=0$ (left panel) and $T/\omega_c=0.01$ (right panel).

Other interesting aspects of our calculations, hinted in the text, concern the question of transport and dissipation in the quantum Hall regime. Although this topic goes far beyond the scope of the present Rapid Communication, we have noted the natural emergence of quantization and lifetime effects in the respective cases of closed and open systems from the simple dynamics of equipotentials lines given by Eq. (7). Further developments of this idea may be useful in bringing together a better understanding of local excitations and macroscopic transport properties of quantum Hall fluids.

[1] K. von Klitzing, Philos. Trans. R. Soc. London, Ser. A **363**, 2203 (2005).

[2] S. Ilani, J. Martin, E. Teitelbaum, J. H. Smet, D. Mahalu, V. Umansky, and A. Yacoby, Nature (London) **427**, 328 (2004).

[3] K. Hashimoto, C. Sohrmann, J. Wiebe, T. Inaoka, F. Meier, Y. Hirayama, R. A. Romer, R. Wiesendanger, and M. Morgenstern, Phys. Rev. Lett. **101**, 256802 (2008).

[4] T. Champel and S. Florens, Phys. Rev. B **75**, 245326 (2007).

[5] T. Champel, S. Florens, and L. Canet, Phys. Rev. B **78**, 125302 (2008).

[6] We now set Boltzmann's constant and $\hbar$ to unity, so that energy, temperature, and frequency are equivalently used.

[7] T. Champel and S. Florens, Phys. Rev. B **80**, 125322 (2009).

[8] A. Entelis and S. Levit, Phys. Rev. Lett. **69**, 3001 (1992).

[9] S. A. Trugman, Phys. Rev. B **27**, 7539 (1983).

[10] S. M. Girvin and T. Jach, Phys. Rev. B **29**, 5617 (1984).

[11] J. K. Jain and S. Kivelson, Phys. Rev. B **37**, 4111 (1988).

[12] H. A. Fertig and B. I. Halperin, Phys. Rev. B **36**, 7969 (1987).

[13] *Handbook of Mathematical Functions*, edited by M. Abramowitz and I. A. Stegun (Dover, New York, 1972).